



Adsorption properties of iron-loaded composite resin for chromium (VI)

Xu Zhang^{a,b}, Wenhong Li^{a,b,*}, Dong Li^{a,b}, Yong Gang^{a,b}

^aSchool of Chemical Engineering, Northwest University, Xi'an, Shaanxi 710069, China, Tel. +86 17765819379; email: 1115434768@qq.com (W. Li), Tel. +86 13679279708; email: zhangxu203@stumail.nwu.edu.cn (X. Zhang), emails: 1641832137@qq.com (D. Li), 1241649695@qq.com (Y. Gang)

^bShaanxi Research Center of Chemical Engineering Technology for Resource Utilization, Xi'an 710069, China

Received 21 May 2018; Accepted 21 November 2018

ABSTRACT

Removal of Cr(VI) from liquid by iron-loaded composite resin was studied. The isothermal adsorption model and the adsorption kinetic model were established. The adsorption thermodynamic parameters were solved. The iron-loaded composite resins before and after adsorption were characterized by scanning electron microscope (SEM) and energy dispersive spectrometer (EDS). It was found that the adsorption capacity of iron-loaded composite resin was higher than others. The results showed that the optimum adsorption condition was performed at 318 K, the pH of 2, and the time of 6 h. Freundlich model and pseudo-first-order kinetic model fitted the experimental data. The main control step of the adsorption was liquid film diffusion process. The value of ΔH was 2–16 kJ mol⁻¹, which showed that the adsorption was an endothermic process. The adsorption of ΔG was less than zero which indicated the adsorption was spontaneous. The value of ΔS was constant positive that revealed the adsorption was the total entropy-increasing process. SEM and EDS analyses indicated that Cr(VI) can adsorb by iron-loaded composite resin effectively. The eluent of 6% NaOH + 5% NaCl had an excellent desorbing performance.

Keywords: Iron-loaded composite resin; Isothermal adsorption model; Adsorption kinetics model; Thermodynamic parameters; Characterization

1. Introduction

Chromium compounds are indispensable raw materials for metallurgy, electroplating, dyestuff, leather making, pharmaceutical industry, and other industrial production processes [1]. There are mainly two common valence states of chromium in solution, namely, Cr(VI) and Cr(III). But their toxicity is quite different. It is reported that the toxicity of Cr(VI) is almost 100 times more than Cr(III) [2]. In addition, Cr(VI) has strong oxidation and high permeability, resulting in irritating, carcinogenic, and mutagenic to human body [3,4]. Nowadays, the harmless treatment of chromium-containing wastewater was studied by scholars, including chemical precipitation method, adsorption method, electrochemical treatment, membrane method, photocatalytic method, biological technology, and combination method [5–11]. Among

these methods, chemical precipitation could produce chromium sludge, electrochemical treatment and membrane method need more energy, and photocatalysis and biological technology have higher costs with poor removal efficiency. However, the adsorption method has been widely used in chemical industries for its good treatment effect, simple operation, and no secondary pollution.

In recent years, the removal of Cr(VI) by adsorption has focused on the preparation of adsorbents, such as oxides and hydroxides with special properties as new adsorbent materials and activated carbon biocomposites prepared from peanut shell, corn cob, walnut shell, etc. [12–16]. Their adsorption capacity ranges from 20 to 100 mg g⁻¹. As an effective adsorbent, ion exchange resin is more favored in the field of adsorption. It is a technology that uses the exchange of ions

* Corresponding author.

on the resin to remove contaminants from water. Its advantage is high selectivity, large adsorption capacity, and strong regeneration. The traditional resin has some limitations in the adsorption of target. Conversely, the modified resin, by adding transition metal elements, cannot only significantly improve the adsorption rate of pollutants but also enhance the advantages of repeated resin regeneration [17,18]. The reason is that electrostatic effect enhances the adsorption capacity of the modified resin.

Thereby, the iron-loaded composite resin was prepared by the anion exchange resin D301 as the carrier and loading Fe^{3+} . The influence of temperature, pH, and time on the adsorption properties was analyzed. The isothermal adsorption model and adsorption kinetic model were established, and the adsorption thermodynamic parameters were solved. Meanwhile, the iron-loaded composite resin before and after adsorption was characterized by energy dispersive spectrometer (EDS) and scanning electron microscope (SEM). Finally, the proportion of mixed eluent was obtained. Compared with others [19–21], iron-loaded composite resin has an excellent performance for bearing Fe. Its adsorption capacity is more than 130 mg g^{-1} , and the desorption effect has unparalleled superiority. It reveals that iron-loaded composite resin is an effective adsorbent for Cr(VI) removal and provides a basis for the preparation and engineering application of the new chromium removal adsorbent.

2. Experiment

2.1. Experimental material

The D301 resins were purchased from Xi'an Sunresin New Materials Co., Ltd (China). Iron trichloride and potassium dichromate were purchased from Sinopharm Chemical Reagent Co., Ltd (China). Sodium hydroxide, hydrochloric acid, sulphuric acid, sodium chloride, and ethanol were purchased from Xi'an Chemical Reagents Factory (China). Diphenyl carbazide was purchased from Tianjin Kemiou Chemical Reagent Co., Ltd (China).

2.2. Experimental methods

2.2.1. Pretreatment of D301 resin

D301 resin was immersed for 6 h in 5 wt. % sodium hydroxide solution and cleaned several times with deionized water. Then, D301 resin was immersed for 6 h in 5 wt. % hydrochloric acid solution and cleaned it to neutral with deionized water. Finally, D301 resin was put into the drying box at the constant temperature of 45°C .

2.2.2. Preparation of iron-loaded composite resin

FeCl_3 solution of 2 g L^{-1} was added to 10 g D301 resin that pretreated in section of 2.2.1. And the mixture is placed in the oscillator under constant temperature for 8 h. In this process, the pH of 2 keeping 2 h, which could depress the production of $\text{Fe}(\text{OH})_3$ precipitation. Then, the pH was adjusted to 8 and 13 for 3 h. It can ensure Fe^{3+} and nitrogen atoms of tertiary amino group form the coordination bond. The upper liquid was filtered through the process of static

and aging and then washed several times with HCl solution, NaOH solution 95 wt. %, and ethanol solution. Finally, it was put into the drying box at the constant temperature of 100°C .

2.2.3. Static adsorption experiment

The different concentrations of Cr(VI) solution were prepared with pH of 2. Then, the pretreatment of resin of 0.1 g was added 100 mL solution and put it into the constant temperature oscillator for 6 h. Finally, the concentration of Cr(VI) in the solution was measured.

2.3. Analysis methods

2.3.1. Drawing of standard curve

Chromium standard reagent with concentration of 1 g L^{-1} was added to the volumetric flasks with capacities 0.00, 2.00, 4.00, 6.00, 8.00, and 10.00 mL. Then, 5 mL of 50 wt. % H_2SO_4 and 2 mL of diphenyl carbazide were added. Finally, deionized water was fixed to scale, and the absorbance was measured. The standard curve equation is as shown in Eq. (1).

$$y = 0.1378x + 0.0093 \quad (1)$$

where x (mL^{-1}) is the concentration and y is the corresponding absorbance.

The R^2 fitted by linear equation is 0.9992, indicating that the equation can be used to determine the concentration of Cr(VI).

2.3.2. Determination of Cr(VI) concentration

A proper amount of solution and 2 mL of diphenyl carbazide were taken into volumetric flask. Constant volume was diluted with deionized water and kept static for 15 min. Then the absorbance was determined and the concentration of Cr(VI) in the solution was calculated by Eq. (1).

2.3.3. Calculation of adsorption quantity

$$Q_e = (C_0 - C_e) \times \frac{V}{m} \quad (2)$$

where Q_e (mg g^{-1}) is the equilibrium adsorption amount, C_0 (mg L^{-1}) is the concentration of Cr(VI) in the initial solution, C_e (mg L^{-1}) is the concentration of Cr(VI) in the solution during adsorption equilibrium, V (mL) is the volume of the solution, and m (g) is the quality of the iron-loaded composite resin.

3. Results and discussion

3.1. The influence of temperature on the adsorption effect

3.1.1. Drawing of adsorption isotherms

The adsorption isotherms were measured at 298, 308, and 318 K, where C_0 was 100, 200, 300, 400, and 500 mg L^{-1} . The result is shown in Fig. 1. With the increase of temperature, the equilibrium adsorption amount of Cr(VI) in the

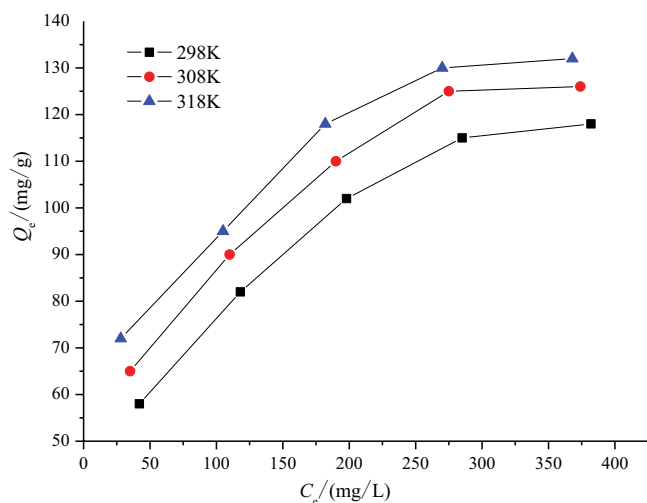


Fig. 1. Adsorption isotherms at different temperatures.

solution increased gradually, indicating that the higher temperature was beneficial to the adsorption process and the adsorption was endothermic process [22,23]. The equilibrium adsorption capacity increased with the increase of the equilibrium concentration of Cr(VI) in the solution and then gradually becomes gentle. That is because with the increase of the equilibrium concentration, the number of Cr(VI) ions increases, which in turn gradually increases the adsorption capacity of the resin. If the equilibrium concentration of Cr(VI) increases, the adsorption capacity of iron-loaded composite resin will reach the limit. When the temperature was 318 K, the maximum adsorption capacity of iron-loaded composite resin was 132 mg g⁻¹, which was higher than others.

Additionally, according to the trend of adsorption isotherm, the adsorption showed monolayer adsorption of Cr(VI) [24]. For this reason, the Langmuir model and Freundlich model were chosen and established in the next section.

3.1.2. Establishment of isothermal adsorption model

The Langmuir model assumes that the adsorption is a monolayer adsorption process, the adsorbate is evenly distributed on the surface of the adsorbed material, and the adsorbate has no interaction between the surface of the adsorbed material. After reaching the adsorption equilibrium, the adsorption rate is equal to the desorption rate. The linear Langmuir equation is presented:

$$\frac{1}{Q_e} = \frac{1}{K_L Q_m C_e} + \frac{1}{Q_m} \quad (3)$$

where Q_m (mg g⁻¹) is the saturated adsorption capacity.

The Freundlich model is an empirical equation. It was proposed on the basis of the Langmuir model and assumed that the adsorption energy of the adsorbent material is uneven. The linear form of the Freundlich model is mentioned:

$$\ln Q_e = n \ln C_e + \ln K_F \quad (4)$$

where K_L (mL mg⁻¹) is the binding constant, n and K_F are Freundlich adsorption characteristic constants.

According to Eqs. (3) and (4), the drawing of linear fitting is shown in Figs. 2 and 3, respectively. The fitting parameters are shown in Table 1.

As shown in Figs. 2 and 3 and Table 1, the correlation coefficient (R^2) fitted by the Freundlich model from 298 to 318 K was higher than that of the Langmuir model. Therefore, under the same experimental conditions, the Freundlich model was more suitable for the adsorption process.

The Freundlich model parameter (K_F) reflects the adsorption capacity of iron-loaded composite resin. The increase of temperature can result in the increase of K_F , which indicated that the higher temperature was beneficial to the adsorption. The parameter decreases (n) with the increase of temperature. It was the result of both solvent driving and adsorbent driving [25,26].

3.2. The influence of pH on the adsorption effect

The effect of pH is an important parameter in the process of adsorption. Adsorption of Cr(VI) was studied in the

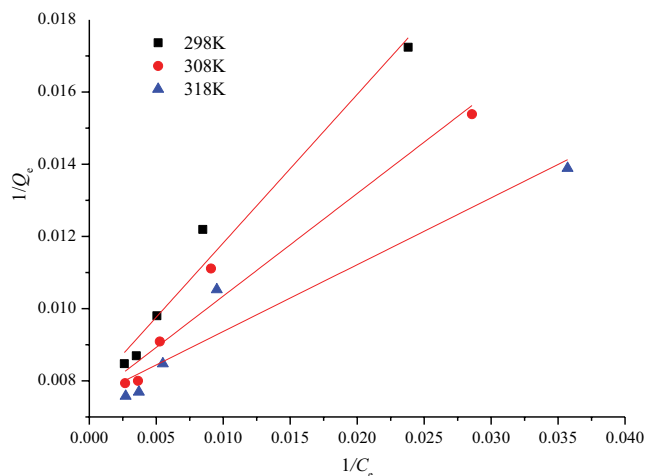


Fig. 2. The linear fitting of Langmuir model.

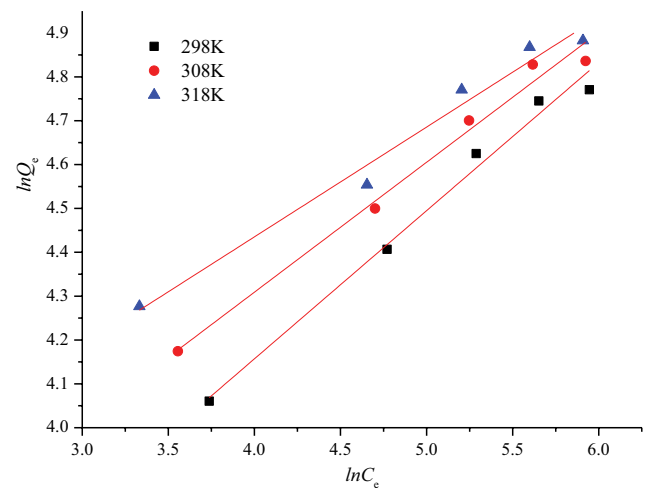


Fig. 3. The linear fitting of Freundlich model.

Table 1
The fitting parameters of Langmuir model and Freundlich model

Model	Temperature (K)	Fitting equation	R^2	K_L (mL·mg ⁻¹)	Q_m (mg·g ⁻¹)
Langmuir	298	$1/Q_e = 0.4114/C_e + 0.0077$	0.9654	0.0187	129.7017
	308	$1/Q_e = 0.2842/C_e + 0.0075$	0.9482	0.0264	133.1558
	318	$1/Q_e = 0.1851/C_e + 0.0075$	0.9022	0.0406	132.9787
Model	Temperature (K)	Fitting equation	R^2	n	K_f
Freundlich	298	$\ln Q_e = 0.3379 \ln C_e + 2.8056$	0.9846	0.3379	16.5373
	308	$\ln Q_e = 0.2962 \ln C_e + 3.1241$	0.9817	0.2962	22.7385
	318	$\ln Q_e = 0.2504 \ln C_e + 3.4337$	0.9736	0.2504	30.9917

pH range of 2–8 when the temperature was 318 K and C_0 was 300 mg L⁻¹. Fig. 4 shows that the equilibrium adsorption of Cr(VI) increases with the decrease in pH. The equilibrium adsorption capacity reaches the maximum with pH of 2. The adsorption effect was the best at this time. A possible explanation for this is as follows [27,28]. Cr(VI) exists in a variety of forms with different pH. At lower pH, the forms of $\text{Cr}_2\text{O}_7^{2-}$ and HCrO_4^- while the main forms of CrO_4^{2-} in higher pH. One $\text{Cr}_2\text{O}_7^{2-}$ or HCrO_4^- ions need one active site, but CrO_4^{2-} ion needs two active sites due to two minus charges of it. Therefore, decreasing the pH value results in an increase in the adsorption efficiency of Cr(VI). Besides, the increase of pH will lead to competitive adsorption and decrease the adsorption capacity. Thus, the optimum adsorption pH was 2.

3.3. The influence of time on the adsorption effect

The effect of time on the adsorption capacity is shown in Fig. 5. With increases in the adsorption time the adsorption capacity of Cr(VI) increases. In the initial time of 4 h, the adsorption capacity increased significantly and then gradually levelled off. When the adsorption time exceeded 6 h, the adsorption capacity remains steady, and the adsorption equilibrium was achieved.

At the initial stage of adsorption, there are many active sites on the surface of the iron-loaded composite resin.

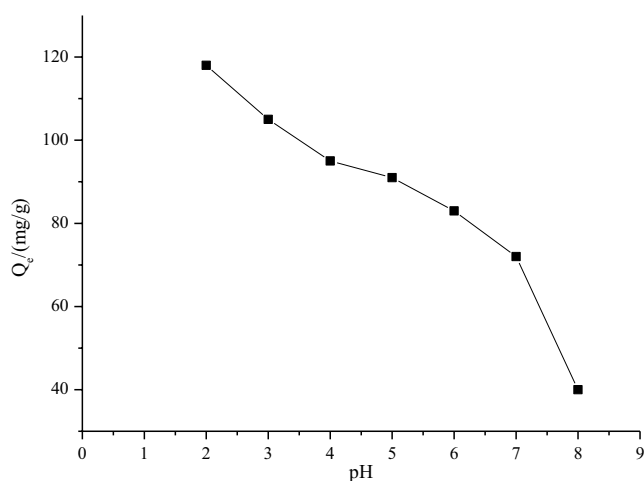


Fig. 4. The effect of pH on adsorption.

The mass transfer force caused by the high concentration difference, so $\text{Cr}_2\text{O}_7^{2-}$ can be easily adsorbed. As time goes on, a large amount of $\text{Cr}_2\text{O}_7^{2-}$ was accumulated on the surface of the iron-loaded composite resin, so the active sites were reduced and the adsorption process was hindered. The adsorption rate was gradually reduced and reached equilibrium, which indicated the adsorption process was monolayer adsorption [29]. Therefore, the optimum adsorption time was 6 h.

3.4. Characterization of iron-loaded composite resin

Fig. 6 shows the SEM of Cr(VI) adsorbed by iron-loaded composite resin. Generally, D301 resin relies on ion exchange between $\text{Cr}_2\text{O}_7^{2-}$ and OH^- to remove Cr(VI); in addition to this effect, the chemical reaction of Fe^{3+} with $\text{Cr}_2\text{O}_7^{2-}$ and the adsorption effect of Fe–O–Fe–Cr (which is produced by Fe–O and $\text{Cr}_2\text{O}_7^{2-}$) increased the removal rate of Cr(VI). It can be seen from Fig. 6 that the surface morphology of the iron-loaded composite resin changed significantly before and after adsorption. A great deal of crystalline and amorphous particles on the surface of the iron-loaded composite resin before adsorption. This was due to the coordination load of transition metal ion Fe^{3+} with D301 resin, which formed a large number of grooves and pores on the surface of D301 resin. It was the microscopic foundation for the adsorption

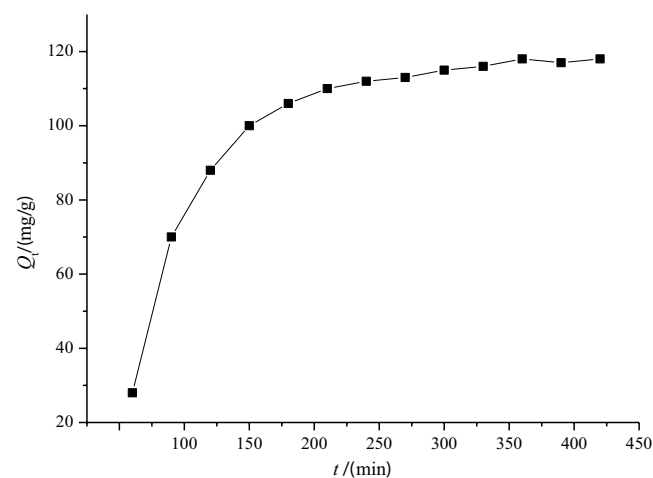


Fig. 5. The influence of time on the adsorption effect (conditions: initial concentration of Cr(VI), 300 mg L⁻¹; pH, 2; temperature, 318 K).

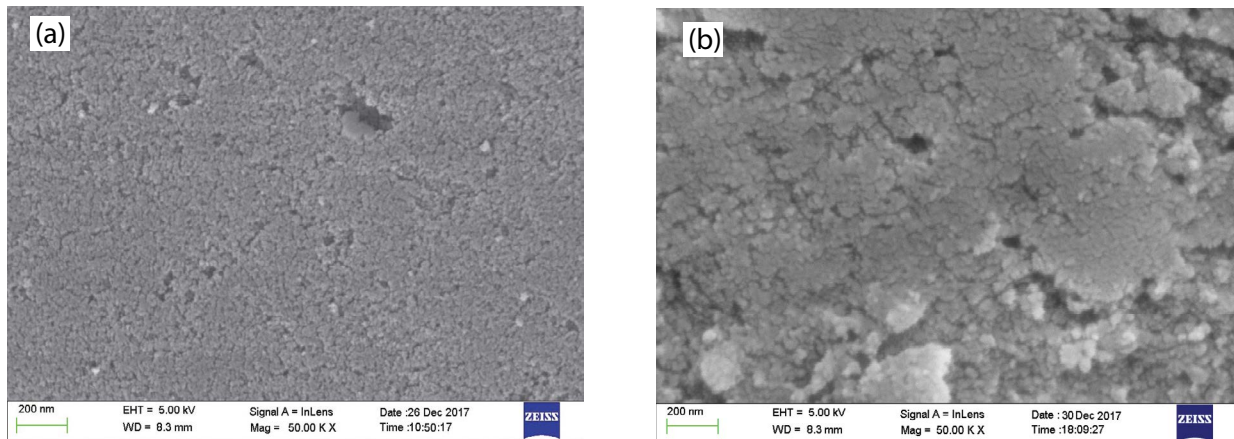


Fig. 6. SEM diagram of iron-loaded composite resin (a) before and (b) after adsorption.

of Cr(VI). When the adsorption was completed, irregular bulk solids appeared on the surface, indicating that Fe^{3+} and $\text{Cr}_2\text{O}_7^{2-}$ deposit on the resin surface. It also showed that the Cr(VI) adsorbed on the surface of the microsphere phase was not entered into the microsphere phase.

EDS analysis indicated that the iron content and chromium content were not detected in D301 resin, but the iron-loaded composite resin they were 4.86% and 0%, respectively. When the adsorption was completed, the iron content of the iron-loaded composite resin was 4.02% and the chromium content was 4.54%. On the one hand, $\text{Cr}_2\text{O}_7^{2-}$ adsorbed on the resin reduced the mass fraction of iron. On the other hand, it was partially removed from the surface of resin due to the chemical precipitation of some iron. Eventually, the iron content of the composite resin was reduced by 0.84%. On the contrary, the increase of chromium content further indicated that the adsorption of Cr(VI) by iron-loaded composite resin has preferable efficiency.

3.5. Establishment of kinetic model of adsorption

Adsorption was accomplished by three steps: liquid film diffusion process, intraparticle diffusion process, and adsorption reaction process. The whole adsorption process may be controlled by one or more steps [30]. Lagergren pseudo-first-order kinetic model, pseudo-second-order kinetic model, and internal diffusion model were applied to establish the kinetic model of adsorption [31]. Three models are shown by the following Eqs. (5)–(7).

$$\ln(Q_e - Q_t) = \ln Q_e - K_1 t \quad (5)$$

$$\frac{t}{Q_t} = \frac{1}{K_2 Q_e^2} + \frac{t}{Q_e} \quad (6)$$

$$Q_t = K_p t^{0.5} + C \quad (7)$$

where Q_t (mg g^{-1}) is the adsorption amount of time, K_1 (min^{-1}) is the first-order kinetic rate constant, K_2 ($\text{g mg}^{-1} \text{min}^{-1}$) is the second-order kinetic rate constant, K_p ($\text{g mg}^{-1} \text{min}^{0.5}$) is the internal diffusion rate constant, and C is constant.

Fig. 7 was obtained by Lagergren model fitting in Fig. 5. The fitting parameters are shown in Table 2. The fitting degree of the pseudo-first-order kinetic equation was better, the correlation coefficient (R^2) was higher than the pseudo-first-order and pseudo-second-order equation, and the parameter (Q_e) of the pseudo-first-order kinetic equation was closer to the experimental value. Consequently, the adsorption process coincided with the pseudo-first-order kinetic equation.

The curve fitted by the internal diffusion model is shown in Fig. 8. The fitting parameters are shown in Table 3. The curve was not a straight line over the origin but a different stage fitting line. Therefore, the adsorption process was not only controlled by liquid film diffusion but also controlled by the intraparticle diffusion [32]. Furthermore, the first stage of K_p was greater than the second stage; we can predict that the liquid film diffusion was the main control step [33].

3.6. Determination of thermodynamic parameters

Thermodynamic parameters (ΔH , ΔS , ΔG) were analyzed to further study the adsorption process. Following are the Eqs. (8)–(10).

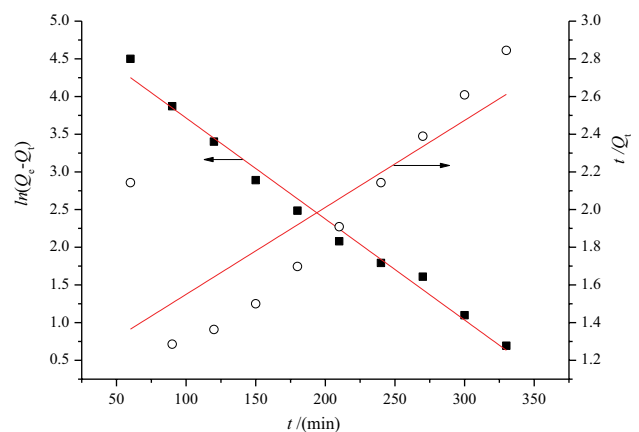


Fig. 7. Fitting results of Lagergren pseudo-first- and second-order kinetic models.

Table 2
The fitting parameters of Lagergren model

Model	Fitting equation	R ²	K	Q _e (mg·g ⁻¹)
Pseudo-first-order kinetic model	ln(159.7920 - Q _t) = -0.0134t + 5.0549	0.9851	0.0134	159.7920
Pseudo-second-order kinetic model	t/Q _t = 0.0046t + 1.0885	0.5756	1.9609 × 10 ⁻⁵	216.4502

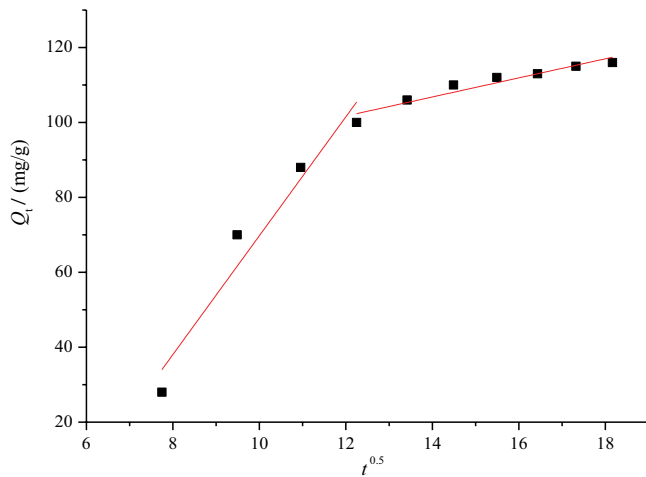


Fig. 8. The fitting result of the internal diffusion model.

Table 3
Fitting parameters of internal diffusion model

Stage	Fitting equation	R ²	K _p	C
First	Q _t = 15.8651t ^{0.5} - 88.8746	0.9269	15.8651	-88.8746
Second	Q _t = 2.5461t ^{0.5} + 71.1620	0.9130	2.5461	71.1620

$$\ln C_e = -\ln K_0 + \frac{\Delta H}{RT} \tag{8}$$

$$\Delta G = -nRT \tag{9}$$

$$\Delta S = \frac{(\Delta H - \Delta G)}{T} \tag{10}$$

where K₀ is constant, R equal 8.314 J mol⁻¹ K⁻¹, and n is Freundlich model parameter.

Table 4
Calculation results of thermodynamic parameters

C ₀ (mg·L ⁻¹)	ΔH (kJ·mol ⁻¹)	ΔG (kJ·mol ⁻¹)			ΔS (J·mol ⁻¹ ·K ⁻¹)		
		298 K	308 K	318 K	298 K	308 K	318 K
100	15.9496				56.3315	54.2470	52.2378
200	4.6066				18.2678	17.4191	16.5680
300	3.3174	-0.8372	-0.7585	-0.6620	13.9416	13.2334	12.5139
400	2.1365				9.9789	9.3993	8.8004
500	1.4725				7.7507	7.2435	6.7123

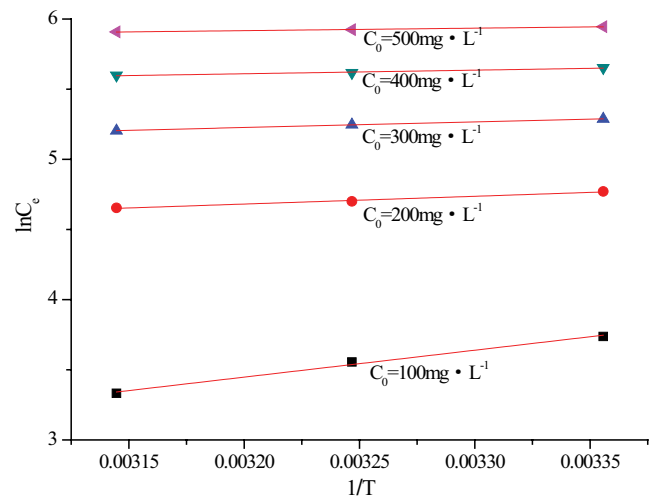


Fig. 9. Fitting results of adsorption enthalpy.

Enthalpy (ΔH) can be fitted and calculated with lnC_e~1/T, as shown in Fig. 9. The results of three parameters are shown in Table 4. In the range of 298–318 K, the value of ΔH was constant and less than 20 kJ mol⁻¹, indicating the adsorption of Cr(VI) was the physical adsorption process. It also confirmed that the adsorption process was endothermic. The constant negative of the ΔG indicated that the adsorption was spontaneous. The ΔS was constant positive because the degree of freedom of the Cr(VI) was reduced after adsorption, but the water molecules were released into the liquid phase to increase the degree of freedom. Finally, it leads to the total entropy increase [34].

3.7. Desorption of iron-loaded composite resin

According to other studies [35,36], desorption rate of the resin can be greatly improved by the mixed eluate. The different mass fraction of NaOH and 5 wt. % NaCl mixed eluent were

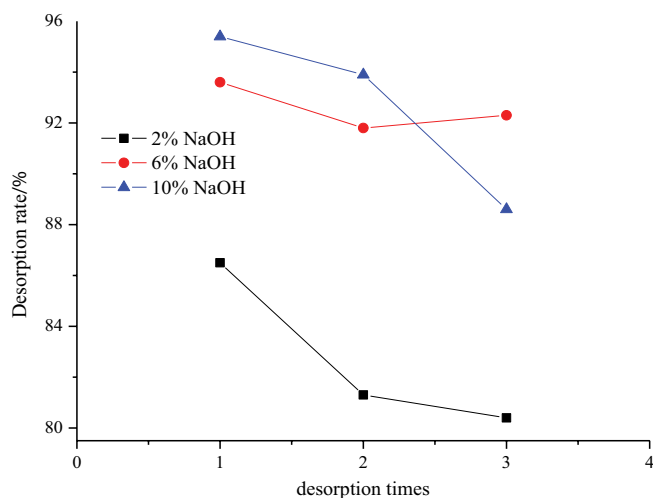


Fig. 10. Effect of NaOH solution with different mass fractions on desorption rate (the ratio of resin to mixed eluent, 0.1 g to 1 mL; temperature, 298 K; time, 2.5 h; number of times, 3).

used to regenerate the iron-loaded composite resin. The results of the experiment were shown in Fig. 10. With the increase of desorption times, the desorption rates of 2% NaOH + 5% NaCl and 10% NaOH + 5% NaCl gradually decrease. However, the range of desorption rate of 6% NaOH + 5% NaCl was 91%–94%. The first two desorption rates of 10% NaOH + 5% NaCl were better than 6% NaOH + 5% NaCl, but as far as recycling of resin is concerned, the latter was more suitable.

4. Conclusion

The optimum conditions for adsorption of Cr(VI) with iron-loaded composite resin were obtained (temperature was 318 K, pH of 2, adsorption time was 6 h). Freundlich model and pseudo-first-order kinetic model were more suitable for the monolayer adsorption process, and the higher temperature was beneficial to the adsorption. The results of SEM and EDS showed that Fe³⁺ bearing iron-loaded composite resin could effectively adsorb Cr(VI). The adsorption process was controlled not only by liquid film diffusion but also by the intraparticle diffusion, and the liquid film diffusion was the main control step. The value of ΔH was constant and less than 20 kJ mol⁻¹, which showed that the adsorption was an endothermic process. The adsorption of ΔG is less than zero that indicated the adsorption was spontaneous. The value of ΔS was constant positive which revealed the adsorption was the total entropy-increasing process. The eluent of 6% NaOH + 5% NaCl had excellent desorbing performance, and the desorption rate was 91%–94%.

Acknowledgements

The authors are grateful to the financial support of the Shaanxi Province Youth Science and Technology Nova Project (project number: 2016KJXX-32), the Overall Science and Technology Innovation Project of Shaanxi Province (project number: 2014KTCL01-09), the Scientific Research Project of the Department of Education of Shaanxi Province (project number: 15JF031)

References

- [1] H.J. Lunk, Discovery, properties and applications of chromium and its compounds, *ChemTexts*, 6 (2015) 1–17.
- [2] N. Misra, V. Kumar, S. Rawat, N.K. Goel, S.A. Shelkar, Jagannath, R.K. Singhal, L. Varshney, Mitigation of Cr(VI) toxicity using Pd-nanoparticles immobilized catalytic reactor (Pd-NiCaR) fabricated via plasma and gamma radiation, *Environ. Sci. Pollut. Res.*, 25 (2018) 16101–16110.
- [3] L.E. Wu, A. Levina, H.H. Harris, Z. Cai, B. Lai, S. Vogt, D.E. James, P.A. Lay, Carcinogenic chromium(VI) compounds formed by intracellular oxidation of chromium(III) dietary supplements by adipocytes, *Angew. Chem. Int. Ed.*, 55 (2016) 1742–1745.
- [4] R. Acharya, B. Naik, K. Parida, Cr(VI) remediation from aqueous environment through modified-TiO₂-mediated photocatalytic reduction, *Beilstein. J. Nanotechnol.*, 9 (2018) 1448–1470.
- [5] B.H. Xie, C. Shan, Z. Xu, X.C. Li, X.L. Zhang, J.J. Chen, B.C. Pan, One-step removal of Cr(VI) at alkaline pH by UV/sulfite process: reduction to Cr(III) and in situ Cr(III) precipitation, *Chem. Eng. J.*, 308 (2017) 791–797.
- [6] C.G. Lee, S. Lee, J.A. Park, C. Park, S.J. Lee, S.B. Kim, B. An, S.T. Yun, S.H. Lee, J.W. Choi, Removal of copper, nickel and chromium mixtures from metal plating wastewater by adsorption with modified carbon foam, *Chemosphere*, 166 (2017) 203–211.
- [7] S.Y. Li, Removal of Cr(VI) from electroplating industry effluent via electrochemical reduction, *Int. J. Electrochem. Sci.*, 13 (2018) 655–663.
- [8] D.D. Xu, J.W. Lu, S. Yan, X. Ru, Aminated EVOH nanofiber membranes for Cr(VI) adsorption from aqueous solution, *RSC Adv.*, 8 (2018) 742–751.
- [9] P. Kar, T.K. Maji, P.K. Sarkar, P. Lemmens, S.K. Pal, Development of a photo-catalytic converter for potential use in the detoxification of Cr(VI) metal in water from natural resources, *J. Mater. Chem. A*, 6 (2018) 3674–3683.
- [10] K.M. Sumathi, S. Mahimairaja, R. Naidu, Use of low-cost biological wastes and vermiculite for removal of chromium from tannery effluent, *Bioresour. Technol.*, 96 (2014) 9–316.
- [11] M.Q. Li, C.F. Yang, K. Zhao, J.Q. Sun, J. Li, L.N. Luo, C.Z. Hu, Removal of Cr(VI) from wastewater by electrocoagulation membrane reactor based on reduction, flocculation and ultrafiltration, *Chin. J. Environ. Eng.*, 12 (2018) 79–85.
- [12] Y. Lu, B. Jiang, L. Fang, F.L. Ling, J.M. Gao, F. Wu, X.H. Zhang, High performance NiFe layered double hydroxide for methyl orange dye and Cr(VI) adsorption, *Chemosphere*, 152 (2016) 415–422.
- [13] C.S. Lei, X.F. Zhu, B.C. Zhu, C.J. Jiang, Y. Le, J.G. Yu, Superb adsorption capacity of hierarchical calcined Ni/Mg/Al layered double hydroxides for Congo red and Cr(VI) ions, *J. Hazard. Mater.*, 321 (2017) 801–811.
- [14] Y.T. Han, C. Xi, O.Y. Xin, P.S. Saran, J.W. Chen, Adsorption kinetics of magnetic biochar derived from peanut hull on removal of Cr(VI) from aqueous solution: Effects of production conditions and particle size, *Chemosphere*, 145 (2016) 336–341.
- [15] S.X. Tang, Y. Chen, R.Z. Xie, W.J. Jiang, Y.X. Jiang, Preparation of activated carbon from corn cob and its adsorption behavior on Cr(VI) removal, *Water Sci. Technol.*, 73 (2016) 2654–2661.
- [16] M. Banerjee, R.K. Basu, S.K. Das, Cr(VI) adsorption by a green adsorbent walnut shell: adsorption studies, regeneration studies, scale-up design and economic feasibility, *Process Saf. Environ.*, 116 (2018) 693–702.
- [17] X.W. Liu, J.H. Chen, J.Q. Chen, Removal of antimony from water by supported iron-zirconium bimetal oxide polymeric anion exchange resin, *Ion Exch. Adsorpt.*, 32 (2016) 244–252.
- [18] X.J. Hu, Y.B. Peng, Y.S. Li, Preparation of thiacalix[4] arenetetrasulfonate-modified D201 resin and its adsorption of heavy metal ions, *Desal. Wat. Treat.*, 57 (2016) 12350–12363.
- [19] R. Coskun, E. Er, A. Delibas, Synthesis of novel resin containing carbamothiolylimidamide group and application for Cr(VI) removal, *Polym. Bull.*, 75 (2017) 963–983.
- [20] Y.Y. Ye, Y.X. Ren, J. Zhu, J.P. Wang, B.Y. Li, Removal of nitrate and Cr(VI) from drinking water by a macroporous anion exchange resin, *Desal. Wat. Treat.*, 57 (2016) 1–13.

- [21] K. Xiao, F.Y. Xu, L.H. Jiang, Z.G. Dan, N. Duan, The oxidative degradation of polystyrene resins on the removal of Cr(VI) from wastewater by anion exchange, *Chemosphere*, 156 (2016) 326–333.
- [22] X.L. Song, H. Qian, X.L. Liu, X. Li, Study on sorption thermodynamics and kinetics of Cr(VI) on ion-exchange resin, *Appl. Chem. Ind.*, 42 (2013) 99–101.
- [23] J.P. Valle, B. Gonzalez, J. Schulz, D. Salinas, U. Romero, D.F. Gonzalez, C. Valdes, J.M. Cantu, T.M. Eubanks, J.G. Parsons, Sorption of Cr(III) and Cr(VI) to $K_2Mn_4O_9$ nanomaterial a study of the effect of pH, time, temperature and interferences, *Microchem. J.*, 133 (2017) 614–621.
- [24] M. Shaban, M.R. Abukhadra, A.A.P. Khan, B.M. Jibali, Removal of Congo red, methylene blue and Cr(VI) ions from water using natural serpentine, *J. Taiwan Inst. Chem. Eng.*, 10 (2017) 1–15.
- [25] L.Z. Xiong, R. Wang, W. Tian, Z.Q. He, Adsorption kinetics and thermodynamics of flavonoids in the leaves of eucommia ulmoides oliv with macroporous adsorption resins, *Ion Exch. Adsorpt.*, 29 (2013) 526–534.
- [26] X.B. Suo, W.Q. Wang, X. Xu, H. Zhang, Adsorption kinetics of ephedrine and pseudo ephedrine on two types of macroporous resins, *Ion Exch. Adsorpt.*, 30 (2014) 350–358.
- [27] J.B. Yang, M.Q. Yu, T. Qiu, Adsorption thermodynamics and kinetics of Cr(VI) on KIP210 resin, *J. Ind. Eng. Chem.*, 20 (2014) 480–486.
- [28] G.D. Zou, J.X. Guo, Q.M. Peng, A.G. Zhou, Q.R. Zhang, B.Z. Liu, Synthesis of urchin-like rutile titania carbon nanocomposites by iron-facilitated phase transformation of MXene for environmental remediation, *J. Mater. Chem. A*, 4 (2015) 489–499.
- [29] P.S. Koujalagi, S.V. Divekar, R.M. Kulkarni, R.K. Nagarale, Kinetics, thermodynamic, and adsorption studies on removal of chromium(VI) using Tulsion A-27(MP) resin, *Desal. Wat. Treat.*, 51 (2013) 3273–3283.
- [30] N. Barka, K. Ouzaouit, M. Abdennouri, M.E. Makhfouk, Dried prickly pear cactus (*Opuntia ficus indica*) cladodes as a low-cost and eco-friendly biosorbent for dyes removal from aqueous solutions, *J. Taiwan Inst. Chem. Eng.*, 44 (2013) 52–60.
- [31] S. Yang, L.Y. Li, Z.G. Pei, C.M. Li, J.T. Lv, J.T. Xie, B. Wen, S.Z. Zhang, Adsorption kinetics, isotherms and thermodynamics of Cr(III) on graphene oxide, *Colloids Surf., A Physicochem. Eng. Asp.*, 457 (2014) 100–106.
- [32] B. Zhang, L.P. Sun, Y.H. Wu, H. Xu, K. Tu, Adsorption kinetics of flavonoids from peanut hull by macroporous resin, *Chin. Oils and Fats*, 42 (2017) 122–126.
- [33] J. Wang, H.J. Lei, Z.Z. Yue, R.X. Gao, K.R. Wang, H.D. Xu, Adsorption characteristics of patulin in jujube juice using macroporous resin, *Trans. Chin. Soc. Agric. Eng.*, 31 (2015) 285–291.
- [34] J.B. Dong, J.B. Wu, J. Yang, W. Song, X.J. Dai, Preparation of high-capacity IDA chelating resin and its adsorption properties, *Chem. J. Chinese U.*, 34 (2013) 714–719.
- [35] B.R. Zhu, J.H. Li, H.Y. Shen, J.D. Li, Y.J. Jiang, Y.B. Wang, C.H. Xiong, Cr(VI) removal from aqueous solutions by a high-capacity strong acid resin D296, *Chem. J. Chinese U.*, 31 (2017) 743–748.
- [36] X.Q. Liu, Y. Li, C. Wang, M. Ji, Comparison study on Cr(VI) removal by anion exchange resins of Amberlite IRA96, D301R, and DEX-Cr: isotherm, kinetics, thermodynamics, and regeneration studies, *Desal. Wat. Treat.*, 55 (2015) 1–11.